

## Structure and phase diagram of high-density water: The role of interstitial molecules

A. Marco Saitta\* and Frédéric Datchi

*Physique des Milieux Condensés, CNRS-UMR 7602, B77, Université Pierre et Marie Curie, F-75252 Paris, France*

(Received 16 April 2002; revised manuscript received 20 November 2002; published 10 February 2003)

The structural transformations occurring to water from the low- to the high-density regimes have been studied by classical molecular dynamics calculations. The local structure is analyzed through a proper choice of the relevant orientational distribution functions. This approach sheds light on the key role played by the interstitial molecules in the second coordination shell and identifies a clear structural fingerprint of high-density water. As a consequence, the analogy between the structure of high-density water and those of high-density ices is evidenced.

DOI: 10.1103/PhysRevE.67.020201

PACS number(s): 61.20.Ja, 61.25.Em

Knowledge of the structural and bonding properties of water is crucial in many problems of physics, chemistry, and biology. In particular, the rationalization of its local structure stands as a key point to the understanding of its anomalous properties. The effect of pressure on the structure and the hydrogen-bond network has been addressed by a variety of experimental and theoretical works in the recent past. X-ray [1] and neutron diffraction experiments [2–5], from which pair-distribution functions (PDF) could be extracted, have revealed that dramatic changes in these PDF's, and more evidently in the oxygen-oxygen PDF, occur at ambient temperature for relatively moderate pressures, typically a few kilobars. A number of theoretical calculations have been able to reproduce these changes, including classical molecular dynamics (MD) simulations [6–9]. Other recent theoretical works have rather focused on the properties of the liquid either in deeply supercooled region [10–12], or at high-temperature [13–15], supercritical [16–18], and even planetary conditions [19].

A recurrent picture has emerged to explain the observed behavior under pressure, that is, two structural forms of water may be distinguished in the (meta)stable liquid, referred as low-density and high-density water (LDW and HDW, respectively) [3]. As the pressure is increased, the system undergoes a continuous transformation from the LDW to the HDW form. This behavior is reminiscent of the liquid-liquid transition and second critical-point conjecture in the highly supercooled liquid, although the relation between the two is unclear yet [20].

At ambient conditions, the structure of water is well described in terms of a dynamical network of hydrogen-bonded tetrahedral cages [21]. As it can be inferred from the oxygen-oxygen PDF  $g_{OO}(r)$ , the second shell of neighbor molecules around a central one [contributing to the second peak in  $g_{OO}(r)$ ] is most probably situated at a distance of 4.5 Å from the central molecule, that is, the distance that one expects if these second-shell molecules are hydrogen bonded to the ones forming the first shell. In HDW, conversely, the second shell of neighbor molecules is thought to collapse onto the first one, as a consequence of the rupture of the H-bond network [3]. This description provides an explanation for the

observed shift towards lower distances of the second peak in  $g_{OO}(r)$ . This picture is, however, not easily rationalized with the fact that the local tetrahedral structure does not show any significant modification neither in the first peak of  $g_{OO}(r)$ , nor in the O-O-O orientational distribution function (ODF), whose single broad peak centered around the typical tetrahedral angle is only marginally affected by pressure. Furthermore, the O-H ··· O distance and angle distributions along an H bond hardly change at all, showing that hydrogen bonds remain strong and strongly directional as pressure increases. In other words, the seemingly preserved local tetrahedral structure should hold not only around a “central” molecule, but also around any of its first neighbors, which in turn seems to be in contrast with the hypothesis of a second-shell collapse. Anticipating our results, we will show in the following that the second peak of the oxygen-oxygen PDF is mainly due to molecules which are not H bonded to any of the first-shell molecules, and are thus referred to as *interstitial* molecules.

In this study, molecular dynamics calculations have been carried out in the 0–15 kbar and 240–500 K pressure-temperature range in the N-P-T ensemble with systems containing 108, 216, or 512 water molecules. Simulation times were in the 0.2–1.0 ns range. The TIP4P model [22] has been employed. Although more and more sophisticated classical potentials are developed [23,24], the TIP4P description of the structural properties is very satisfying when compared to experiments [25], and its predictive power well established [26–28]. Our computed PDF's  $g_{OO}(r)$ ,  $g_{OH}(r)$ , and  $g_{HH}(r)$  are indeed in good agreement with experimental data [29] at ambient conditions, as well as with the existing high-pressure results [1]. In particular, our calculated  $g_{OO}(r)$ 's for HDW and LDW compare very well with the extrapolated ones [3].

The effect of pressure on the structural properties of water has been so far mostly analyzed in terms of the PDF's, on one hand, and coordination number, on the other. The latter is defined as  $n(r) = 4\pi\rho\int r^2 g_{OO}(r) dr$ , where  $\rho$  is the number density. As a matter of fact, the ambient-condition value of  $n(r_{min})$ , calculated up to the first minimum  $r_{min}$  of the PDF, is close to 4, reflecting well the tetrahedral geometry of the first neighbors of a given molecule. As mentioned above, the main effect of pressure on  $g_{OO}(r)$  consists in a gradual shift of its second peak from 4.5 Å to about 3.2 Å. Concomi-

\*Electronic address: ms@pmc.jussieu.fr

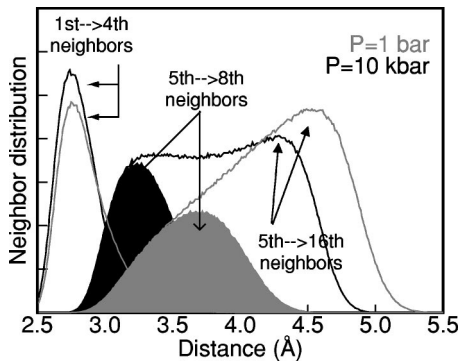


FIG. 1. Distribution at 300 K of the distances to a central molecule of the 1st–4th neighbors, referred to as “first shell,” and of the 5th–16th neighbors, referred to as “second-shell,” at 1 bar (black lines) and 10 kbar (gray lines). The filled regions refer to the 5–8 subshell of the second shell.

tantly, the first minimum of the oxygen-oxygen PDF becomes extremely flat and its exact location rather arbitrary. The coordination number thus becomes ill defined, its estimate being heavily affected by the choice of the cutoff distance. Deeper insights on the local arrangement of molecules cannot therefore be achieved through the analysis of  $g(r)$ , which only yields, by definition, angle-averaged information on the liquid structure. The inclusion of orientational correlations proves instead crucial to the understanding of the effects of pressure on the local structure of water. Very few attempts to take into account three- and higher-body distribution functions have been reported [30] which, in the simplest cases usually considered, do not show any special features. The rigorous study of the ODF's is indeed a formidable task, since five independent angles characterize the relative orientation of two water molecules [31]. We chose to follow a less formal approach to the analysis of the radial and orientational structures: for each molecule and at each configuration, its instantaneous neighbors are ranked and labeled as a function of the distance of its oxygen atom from the oxygen atom of the current central molecule [32]. The oxygen atoms of molecules ranked as 1st–4th neighbors are considered as belonging to the instantaneous first shell of coordination, and labeled as  $O^I$ . Accordingly, oxygens in molecules ranked as 5th–16th neighbors are labeled as  $O^{II}$ . The distribution of distances of the  $O_1$ - $O_4$  and  $O_5$ - $O_{16}$  neighbor shells from a given molecule at 300 K shows that the first one is marginally affected by pressure, only becoming slightly sharper and narrower. The second shell  $O_5$ - $O_{16}$  undergoes a significant change of shape: its single, broad peak at about 4.3 Å at ambient pressure, splits at higher pressures into two peaks (Fig. 1). This suggests that the pressure-induced rearrangement of molecules mainly involves the 5th–8th neighbors subshell, whose probability maximum shifts, at 10 kbar, at about 3.2 Å. As mentioned above, the  $\angle O^I$ - $O$ - $O^I$  angle distribution, peaked at about 105° at ambient conditions, is only moderately affected by pressure, becoming broader, and more pronouncedly shouldered at low angles. This observation does not necessarily imply a major deformation of the tetrahedral cage, being only a consequence of the more and more significant overlap of the first

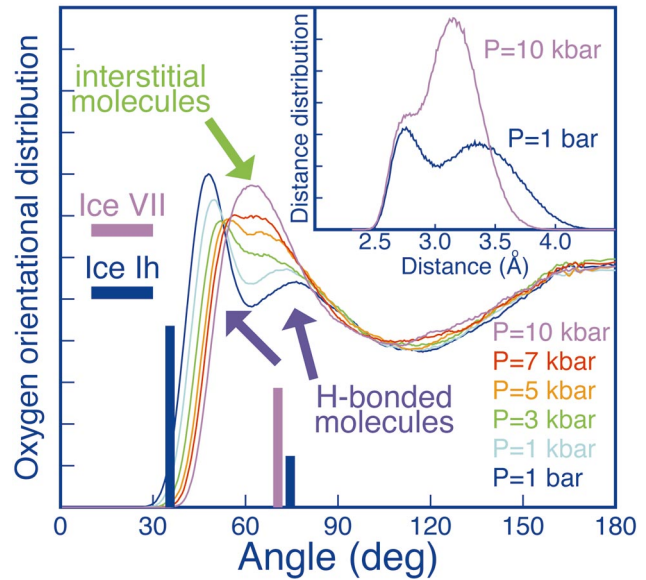


FIG. 2. (Color) Distribution of  $\angle O^I_{1-4}$ - $O$ - $O^{II}_{5-8}$  angles at 300 K and pressures from 1 bar to 10 kbar. Instantaneous neighbors are labeled according to their distance from the central molecule (subscript) and to their shell of coordination (superscript). For example, we refer to  $\angle O_1$ - $O$ - $O_2$  as the angle about an oxygen atom  $O$  formed by its first and second neighbors. The intermolecular separation is chosen as the oxygen-oxygen distance. The effect of pressure is evident in the apparent merging of the two low-pressure peaks into a single one. We report the analogous low-angle peaks observed in ice- $I_h$  and ice-VII. In the inset, we report the distribution of minimal  $\angle O^I$ - $O$ - $O^{II}$  distances for  $\angle O^I_{1-4}$ - $O$ - $O^{II}_{5-8}$  angles around 65° at two different pressures (see text). The second peak, due to interstitial molecules, becomes dominant at high pressure.

and the second shells; molecules labeled as instantaneous first-shell neighbors might often be second-shell neighbors from the structural or chemical point of view. In the  $\angle O^I$ - $O$ - $O^{II}$  angle distribution, shown in Fig. 2, two peaks at about 45° and 75° can be identified at ambient pressure. As represented in Fig. 3, the first peak is due to second-shell molecules which are hydrogen bonded to the  $O^I_i$  atom forming the currently calculated angle, while the second one is due to molecules hydrogen bonded to one of the other three first neighbors  $O^I_{j \neq i}$  to the central molecule. As pressure increases, the two peaks merge into a single one at about 65°. This shift, however, is only apparent, and *does not* correspond to a continuous deformation of the local geometry, and thus to a mere collapse of the second coordination shell. In fact, it reveals that a more profound transformation occurs, and a subtler analysis proves that the structural topology has changed: at high pressure, *other* second-shell molecules are closer to the central one than the second-shell molecules at ambient pressure. In other words, our results show that although the transformation from the low-density to the high-density regime is continuous, this is *not* due to a continuous collapse of the second shell of neighbors onto the first one. Such high-density second-shell molecules are *not* H bonded as their low-density counterparts, but they are purely interstitial. The role of nonbonded molecules, whose importance has been recently confirmed experimentally [5], is supported

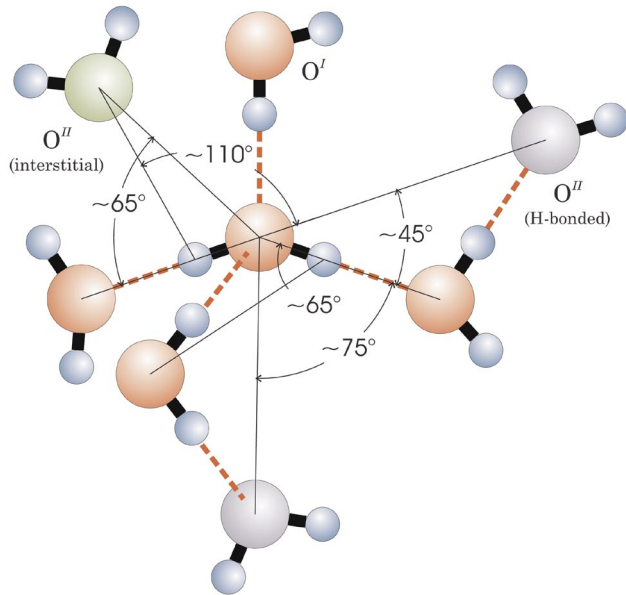


FIG. 3. (Color) Schematic geometry of interstitial and H-bonded water molecules. A water molecule and its first-shell tetrahedral cage are shown with red oxygen atoms; the relevant second-shell neighbors are also reported. In the right part of the sketch, we describe schematically the geometry of molecules belonging to the first shell of coordination of first neighbors to the central molecule. These molecules are referred to as H-bonded molecules, and are displayed with purple oxygen atoms. The two typical LDW  $\angle O^I-O-O^{II}$  angles, as well as the LDW  $\angle O-H-O$  angle described in Fig. 4, are shown. In the upper left corner of the figure, we report the schematic geometry of an interstitial molecule, whose oxygen atom, shown in green, is about 3.2 Å far from both the central molecule and the nearby  $O^I$ , i.e., the typical nonbonded O-O distance. The HDW  $\angle O^I-O-O^{II}$  and  $\angle O-H-O$  angles, at about 65° and 110°, respectively, are shown. Hydrogen bonds (red dashed lines) are represented as perfectly linear for the sake of clarity.

by the study of the distance of the  $O^{II}$  atoms from the three  $O^I_i$  atoms forming the instantaneously closest tetrahedral face. In the inset of Fig. 2, we report the distribution of the shortest distance  $d_{min} = \min[d(O^{II}-O^I_i)]$  for all the  $O^{II}$  atoms contributing to the  $\angle O^I-O-O^{II}$  angle distribution high-density peak at 65°. This distribution, which should reveal the existence of a hydrogen bond between the second-shell oxygen atom  $O^{II}$  and any of the first-shell oxygens  $O^I$ , is double peaked at about 2.8 Å and 3.2 Å. The first peak corresponds indeed to  $O^I-H-O^{II}$  hydrogen bond distances, while the second one is due to non-hydrogen-bonded (i.e., interstitial) second-shell molecules. At ambient pressure, the first peak is the more important one, but higher pressures dramatically enhance the second peak, which is largely dominant beyond 3 kbar. Interestingly, the peak corresponding to hydrogen bonding does not decrease in intensity, showing that second-shell H-bonded molecules maintain a similar contribution to the 65° peak, as other interstitial molecules approach the central one. The role of interstitial molecules in the definition of the structure of HDW emerges even more effectively in the  $\angle O-H-O_2^H$  angle distribution, where O is the intramolecular oxygen and  $O_2^H$  is the first

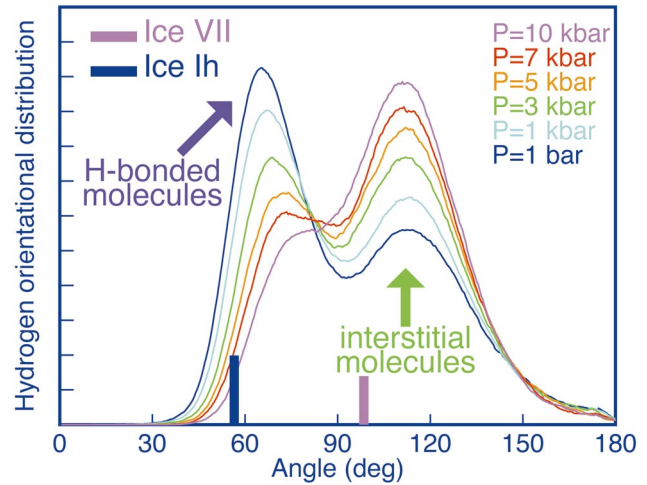


FIG. 4. (Color) Distribution of  $\angle O-H-O_2^H$  angles at 300 K and pressures from 1 bar to 10 kbar. The oxygen of the  $i$ th neighboring molecule to a given hydrogen atom is referred to as  $O_i^H$ ; following this notation, O will be the intramolecular oxygen and  $O_1^H$  the hydrogen-bonded oxygen atom. A dramatic effect of pressure is observed, as the main peak disappears and the second one at 110° increases. By contrast, the  $\angle O-H-O_1^H$  angle distribution is not affected by pressure. We report the analogous peaks observed in ice- $I_h$  and ice-VII.

non-H-bonded neighboring oxygen to the atom H, that is, its third overall O neighbor. This distribution, shown in Fig. 4, unveils a two-state-like geometry: at ambient pressure, the main peak of this distribution at about 65° corresponds to the case of  $O_2^H$  belonging, through a different hydrogen bond, to the tetrahedral cage of the central oxygen O. A smaller peak is observed at about 110°. At high pressure, the second peak

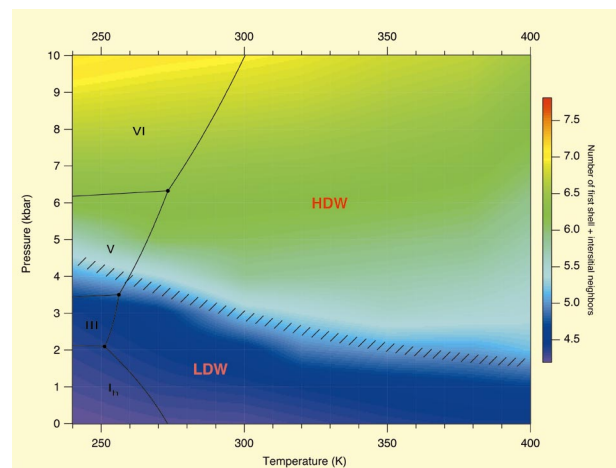


FIG. 5. (Color) Phase diagram of liquid water in the  $P$ - $T$  range considered. The hatched region corresponds to the domain where interstitial and H-bonded second-shell molecules have equal contributions to the  $\angle O-H-O_2^H$  angle distribution. An empirical estimate of the coordination number of first-shell and interstitial molecules is reported. It corresponds to the rigorous definition in the low-density regime, while a distance cutoff at 3.4 Å is chosen for HDW. The domains of the thermodynamically stable phases of ice are also represented.

becomes rapidly more and more pronounced, as the first one disappears; both peak positions seem to have a minor dependence on pressure. The analysis of distance distributions, similar to the one previously described, shows that the second peak, as displayed in the sketch of Fig. 3, is the structural fingerprint of interstitial molecules, which can only approach the central molecule from a very narrow and specific range of directions with respect to the first-shell tetrahedral cage. This double-peaked distribution provides both the onset and the structure of the high-density regime. The former can thus be unambiguously defined in correspondence of the pressure at which the peak due to interstitial molecules overcomes the other one, and is determined in the whole temperature range considered. In Fig. 5, we show the resulting phase diagram of liquid water in the region of thermodynamic stability. Water should be considered in the high-density regime beyond 2.9 kbar at 300 K. This pressure threshold increases at lower temperatures, up to 4.6 kbar at 240 K. We stress at this moment that, in the temperature range of (meta)stability of the liquid phase, there is not a phase transition in the thermodynamic sense between these two forms of water, as they transform continuously one into the other. On the other hand, their domains of existence are presently determined along with the identification and characterization of the HDW structure. A reasonable guess of the HDW resulting average geometry can be formulated. The

structure factor of HDW is known to be remarkably close to the one of the high-density amorphous phase [9], while small but qualitatively important differences are observed between LDW and the low-density amorphous phase [12]. On the other hand, the HDW geometry has been described as locally being close to the local structure of ice-VI or ice-VII, both having interpenetrating tetrahedral networks [33]. Our above structural analysis shows that the oxygen atoms of the 5th–8th neighboring molecules tend to arrange on average at the vertices of two trapezia lying on the two perpendicular  $O_i^l-O-O_j^l$  (instantaneous) planes. This molecular arrangement is indeed locally rather similar to the structure of ice-VII, where the centers of mass of the eight first neighbors occupy the vertices of two perpendicular rectangles.

In conclusion, we carried out MD simulations of water in its  $P$ - $T$  domain of stability and beyond. Our analysis in terms of neighbors and relevant orientational distribution functions shows that it is possible to identify unambiguously the fingerprint of the HDW regime. Moreover, we show that the structure of HDW can be understood in terms of the interstitial second-shell molecules, and seems to be precursor of the structure of high-density ices. Finally, we suggest that the role of such molecules at much lower temperatures should not be overlooked, since it might help to clarify the current debates on the liquid-liquid and amorphous-amorphous phase transitions.

- 
- [1] A.V. Okhulkov, Y.N. Demianets, and Y.E. Gorbaty, *J. Chem. Phys.* **100**, 1578 (1994).
- [2] M.-C. Bellissent-Funel, *Europhys. Lett.* **42**, 161 (1998).
- [3] A.K. Soper and M.A. Ricci, *Phys. Rev. Lett.* **84**, 2881 (2000).
- [4] A.K. Soper, F. Bruni, and M.A. Ricci, *J. Chem. Phys.* **106**, 247 (1997).
- [5] J.L. Finney, A. Hallbrucker, I. Kohl, A.K. Soper, and D.T. Bowron, *Phys. Rev. Lett.* **88**, 225503 (2002).
- [6] J.S. Tse and M.L. Klein, *J. Phys. Chem.* **92**, 315 (1988).
- [7] F. Sciortino, A. Geiger, and H. Stanley, *Phys. Rev. Lett.* **65**, 3452 (1990).
- [8] K. Bagchi, S. Balasubramanian, and M.L. Klein, *J. Chem. Phys.* **107**, 8561 (1997).
- [9] F.W. Starr, M.-C. Bellissent-Funel, and H.E. Stanley, *Phys. Rev. E* **60**, 1084 (1999).
- [10] H. Tanaka, *Phys. Rev. Lett.* **80**, 113 (1998).
- [11] S. Harrington, R. Zhang, P. Poole, F. Sciortino, and H. Stanley, *Phys. Rev. Lett.* **78**, 2409 (1997).
- [12] V.P. Shpakov, P.M. Rodger, J.S. Tse, D.D. Klug, and V.R. Belosludov, *Phys. Rev. Lett.* **88**, 155502 (2002).
- [13] J. Brodholt and B. Wood, *J. Geophys. Res.* **98**, 519 (1993).
- [14] E. Schwegler, G. Galli, and F. Gygi, *Phys. Rev. Lett.* **84**, 2429 (2000).
- [15] E. Schwegler, G. Galli, F. Gygi, and R.Q. Hood, *Phys. Rev. Lett.* **87**, 265501 (2001).
- [16] M. Boero, K. Terakura, T. Ikeshoji, C.C. Liew, and M. Parrinello, *Phys. Rev. Lett.* **85**, 3245 (2000).
- [17] T. Tassaing, M.-C. Bellissent-Funel, B. Guillot, and Y. Guissani, *Europhys. Lett.* **42**, 265 (1998).
- [18] P. Jedlovsky, J.P. Brodholt, F. Bruni, M. Ricci, A.K. Soper, and R. Vallauri, *J. Chem. Phys.* **108**, 8528 (1998).
- [19] C. Cavazzoni, G.L. Chiarotti, S. Scandolo, E. Tosatti, M. Bernasconi, and M. Parrinello, *Science* **283**, 44 (1999).
- [20] O. Mishima and H.E. Stanley, *Nature (London)* **396**, 329 (1998).
- [21] D. Eisenberg and W. Kauzmann, *The Structure and Properties of Water* (Oxford University Press, Oxford, 1969).
- [22] W.L. Jorgensen, J. Chandrasekhar, J.D. Madura, R.W. Impey, and M.L. Klein, *J. Chem. Phys.* **79**, 926 (1983).
- [23] M. Mahoney and W. Jorgensen, *J. Chem. Phys.* **112**, 8910 (2000).
- [24] B. Guillot and Y. Guissani, *J. Chem. Phys.* **114**, 6720 (2001).
- [25] J.M. Sorenson, G. Hura, R.M. Glaeser, and T. Head-Gordon, *J. Chem. Phys.* **113**, 9149 (2000).
- [26] O. Mishima, L.D. Calvert, and E. Whalley, *Nature (London)* **310**, 393 (1984).
- [27] J. Errington and P. Debenedetti, *Nature (London)* **409**, 318 (2001).
- [28] K. Koga, H. Tanaka, and X. Zeng, *Nature (London)* **408**, 546 (2000).
- [29] G. Hura, J.M. Sorenson, R.M. Glaeser, and T. Head-Gordon, *J. Chem. Phys.* **113**, 9140 (2000).
- [30] A.K. Soper, *J. Chem. Phys.* **101**, 6888 (1994).
- [31] T. Lazaridis and M. Karplus, *J. Chem. Phys.* **105**, 4294 (1996).
- [32] S. Mazur, *J. Chem. Phys.* **97**, 9276 (1992).
- [33] M. Canpolat, F.W. Starr, A. Scala, M. Sadr-Lahijany, O. Mishima, S. Havlin, and H.E. Stanley, *Chem. Phys. Lett.* **294**, 9 (1998).